UCLA

AE134: Optical probing of simultaneous Biermann battery and Weibel instability generated magnetic fields in over critical density plasma

27th Annual ATF Users' Meeting
April 30th, 2025

Chan Joshi*, Chaojie Zhang*, Audrey Farrell†, Mitchell Sinclair, Ken Marsh
*PIs, †Presenter

Funding Sources (Concluded):
NSF Grant No. 2003354:003
DOE Grant No. DE-SC0010064
Funding Sources (Active):
UCLA Dean's Office

Experiment Goals

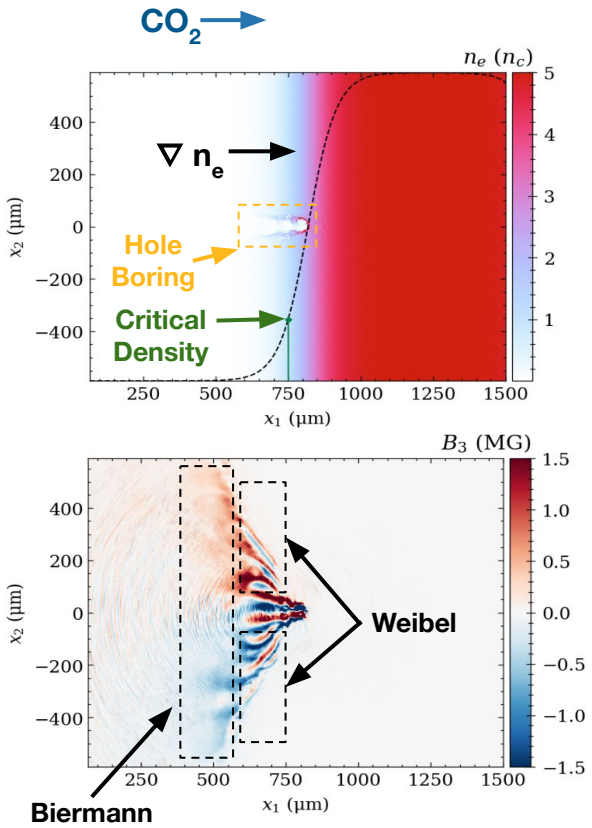

Many mechanisms can generate magnetic fields in high density laser-driven plasmas. These are difficult to measure in solid targets.

- Optically probe overdense laser-plasma interactions relevant to solid density targets using a gaseous target and CO_2 laser driver
- Observe for the first time the coexistence of Biermann battery and Weibel instability generated magnetic fields in a single plasma
- Characterize the conditions in which each mechanism dominates the magnetic field structure

See also [Shukla et al., *Phys. Rev. Research* 2, 023129 (2020)]

Experiment Overview

Our first 3-week experimental campaign took place July 1-19th, 2024.

The experiment involves two primary diagnostics: a wavefront sensor to measure plasma density, and an imaging polarimeter to measure polarization rotation due to magnetic fields in the plasma.

$$\phi_{\mathrm{rot}} = \frac{e}{2m_e c n_c^{\mathrm{probe}}} \int_{\mathcal{P}} n_e \vec{B}_\varphi \cdot d\vec{\ell}$$

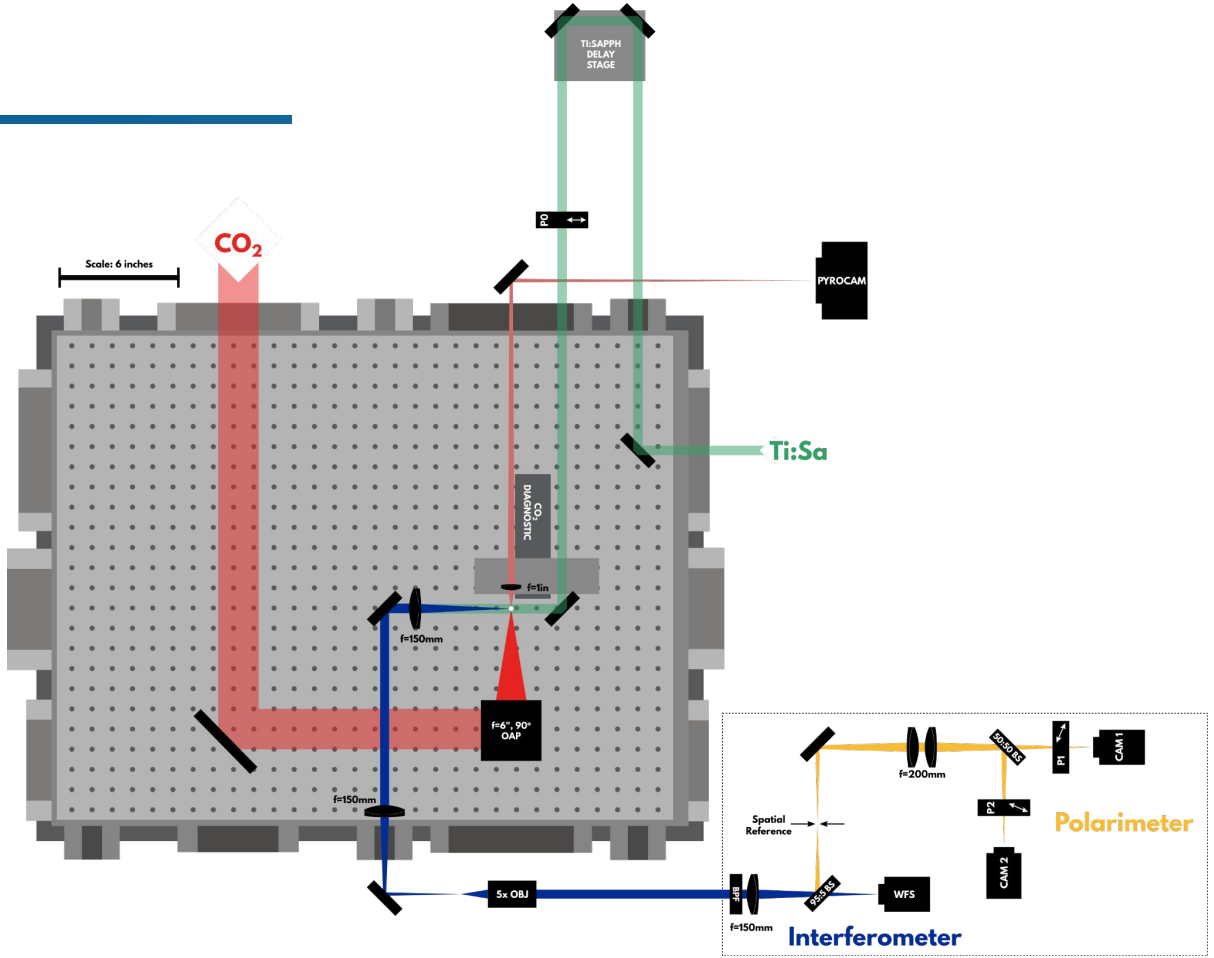

Experiment Overview

Our first 3-week experimental campaign took place July 1-19th, 2024.

The experiment involves two primary diagnostics: a wavefront sensor to measure plasma density, and an imaging polarimeter to measure polarization rotation due to magnetic fields in the plasma.

$$\phi_{\mathrm{rot}} = \frac{e}{2m_e c n_c^{\mathrm{probe}}} \int_{\mathcal{P}} n_e \vec{B}_\varphi \cdot d\vec{\ell}$$

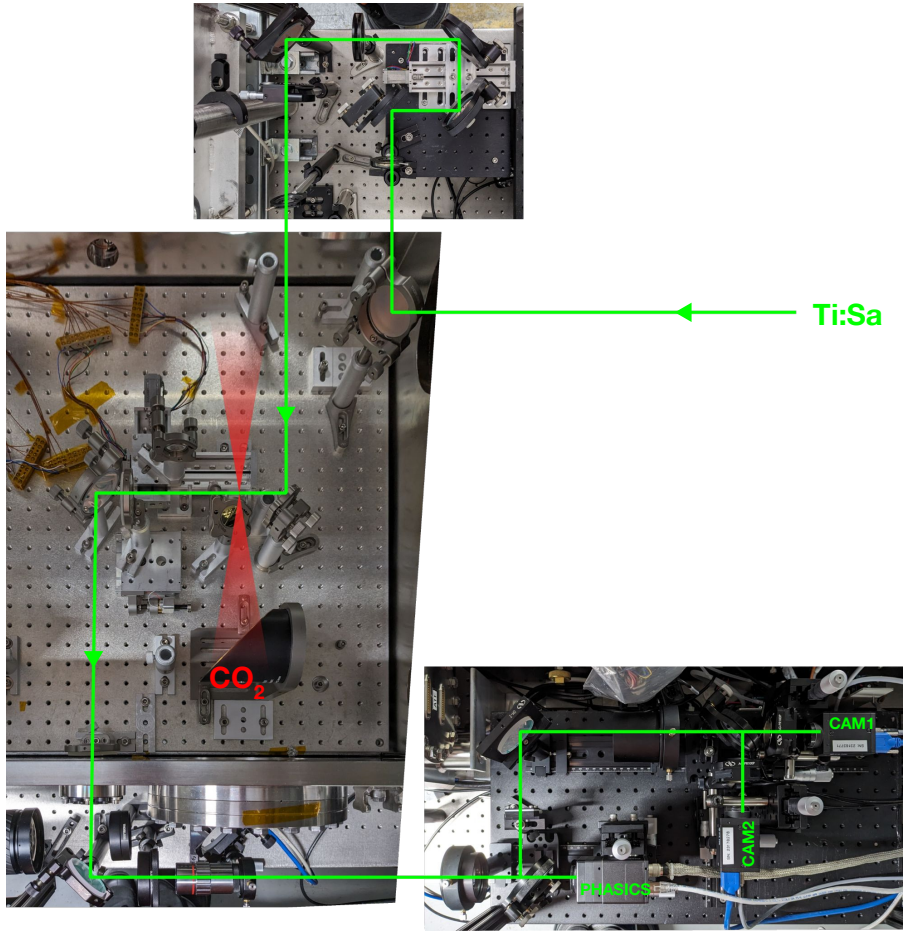

Ionizing multiple nitrogen electrons reaches over critical density.

For our laser parameters up to 5 of nitrogen's electrons can be ionized around the laser focus. For the backing pressure and nozzle position used, this reaches a peak density of $5 \cdot 10^{19} cm^{-3}$.

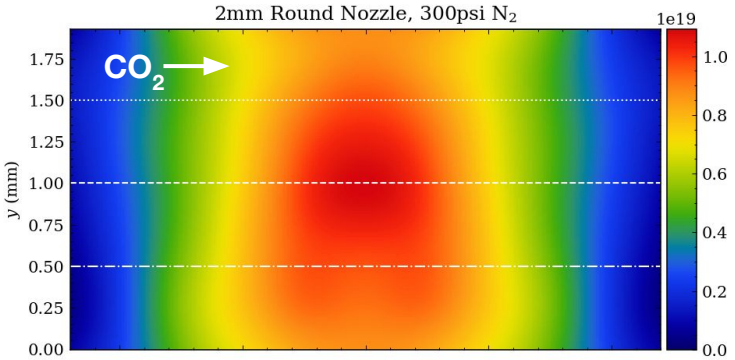

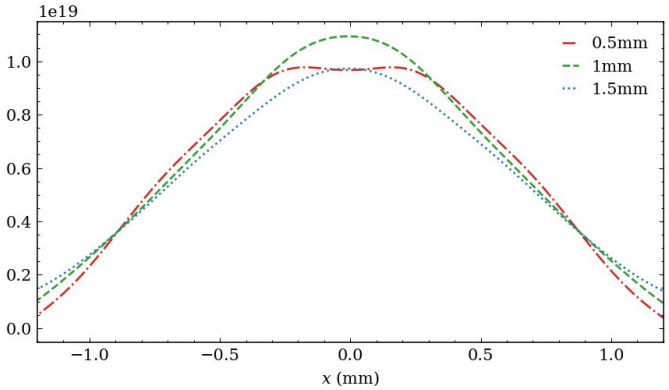

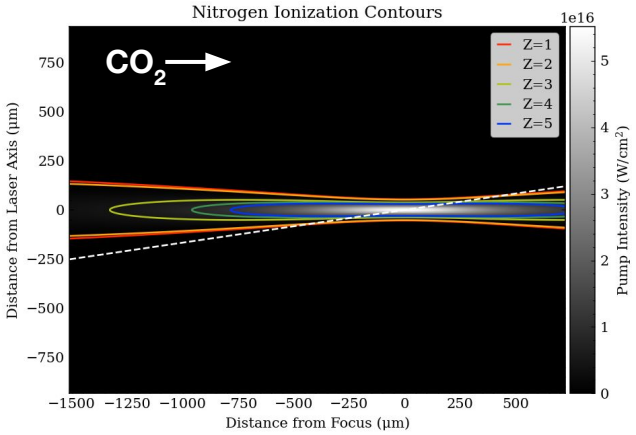

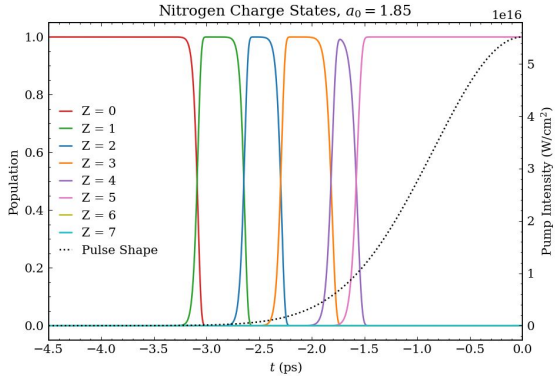

Filaments dominate the density and Faraday rotation data we have.

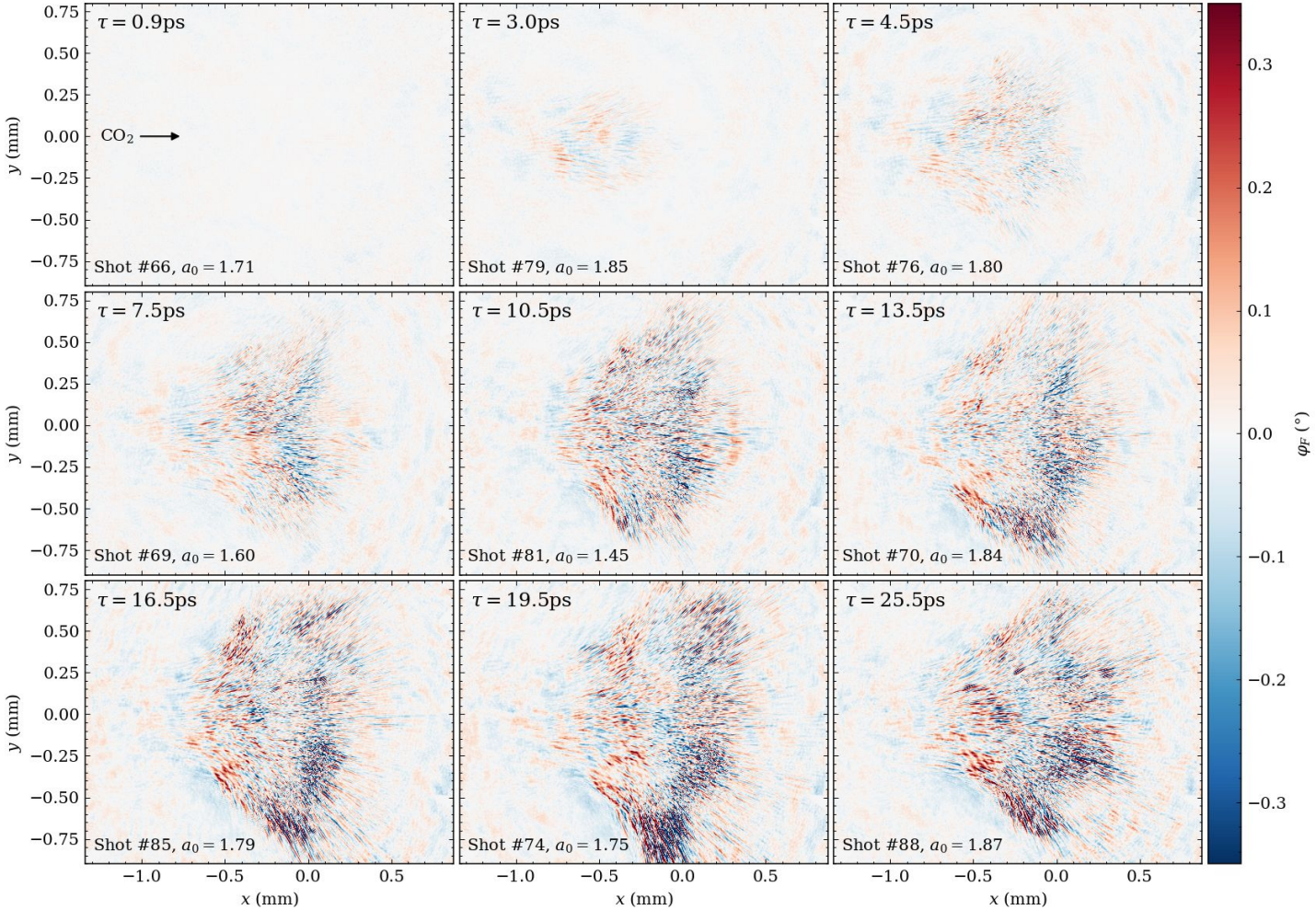

Filaments dominate the density and Faraday rotation data we have.

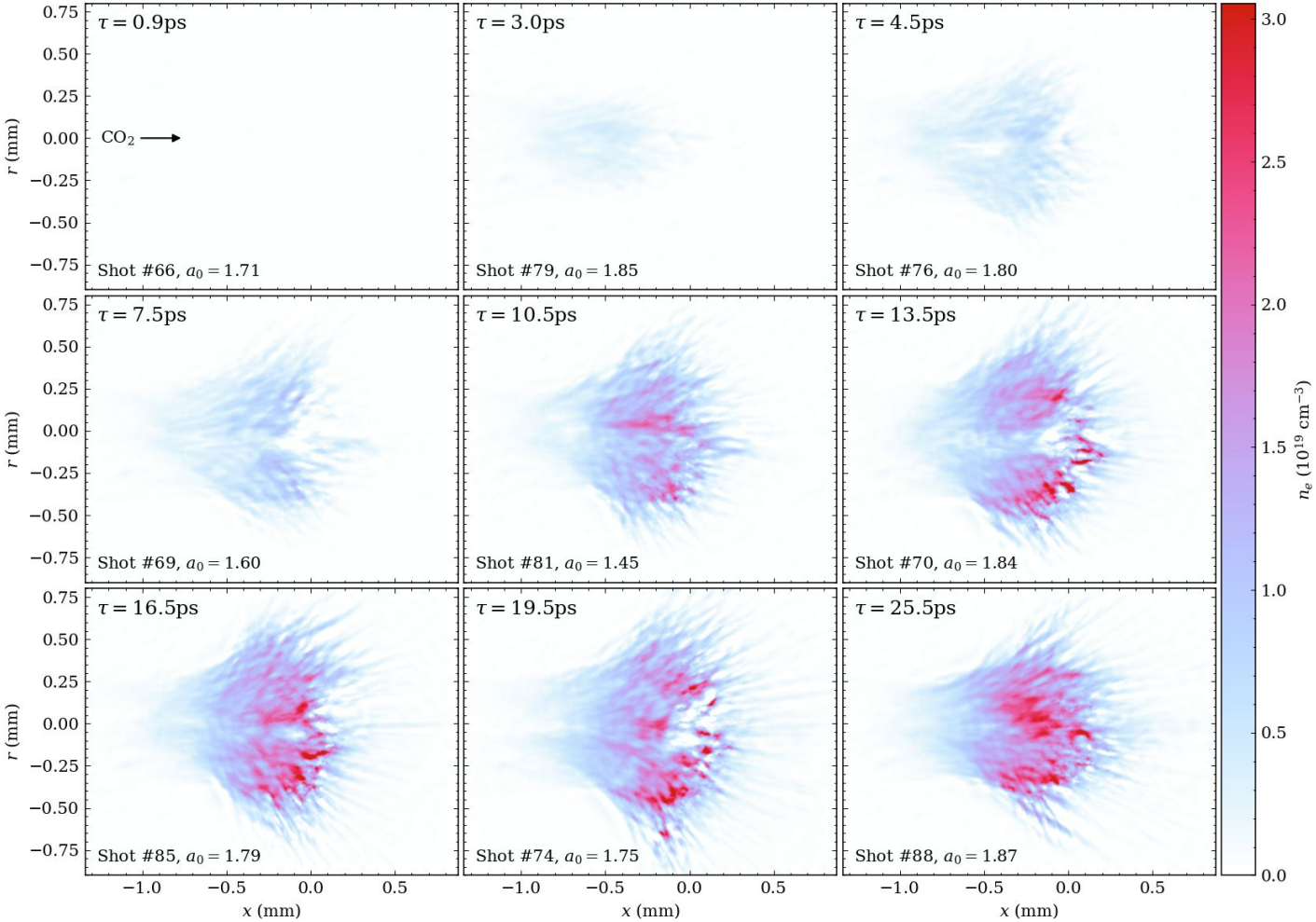

These filaments persist for hundreds of picoseconds.

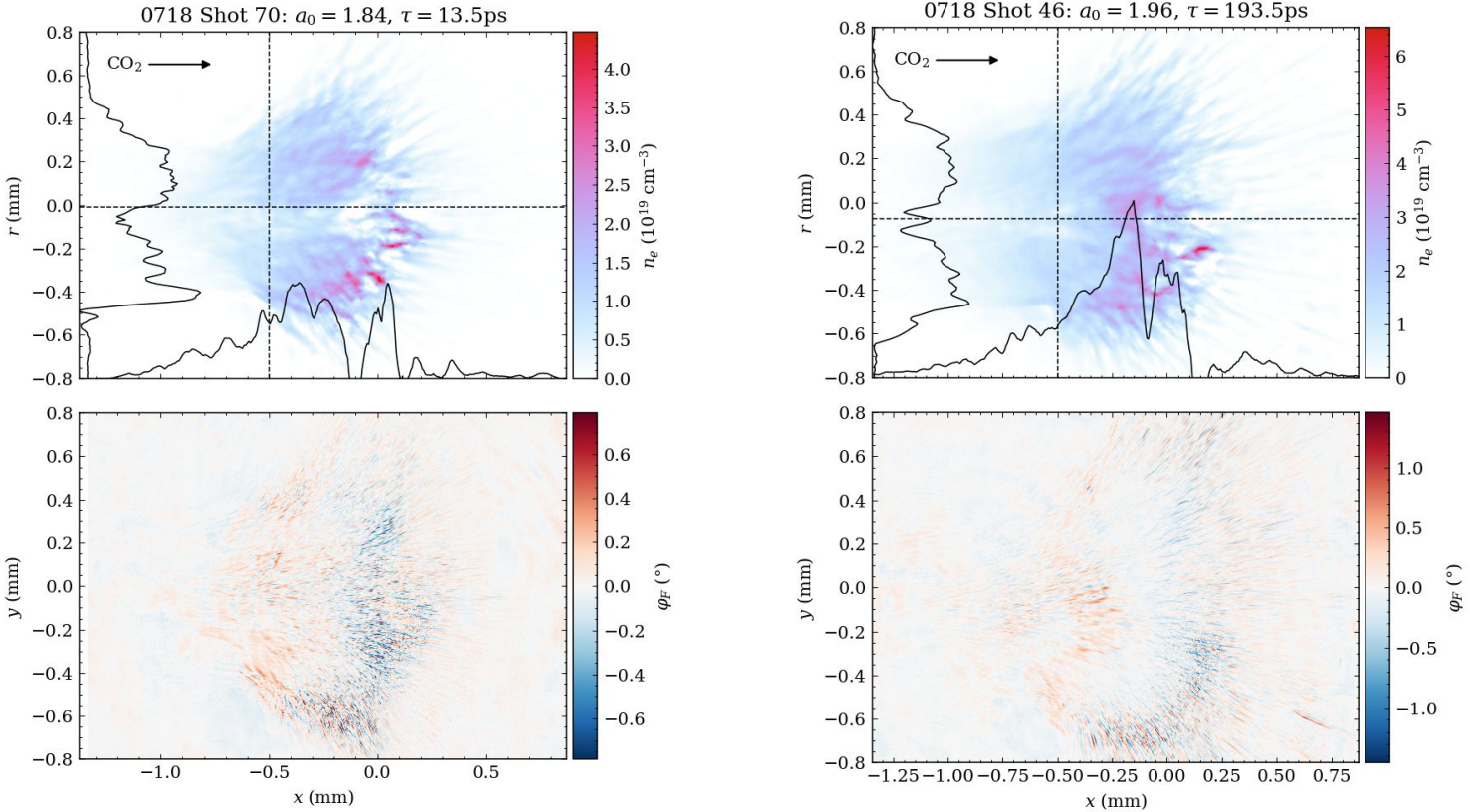

There are some regions which resemble Biermann at early times.

There is some indication of the macroscopic Biermann lobes on the front of the plasma in the Faraday rotation data, particularly at early times. However the signal is very weak due to the low density.

Given the long density gradient scale length, the magnetic fields are expected to be dominated by filamentation rather than Biermann.

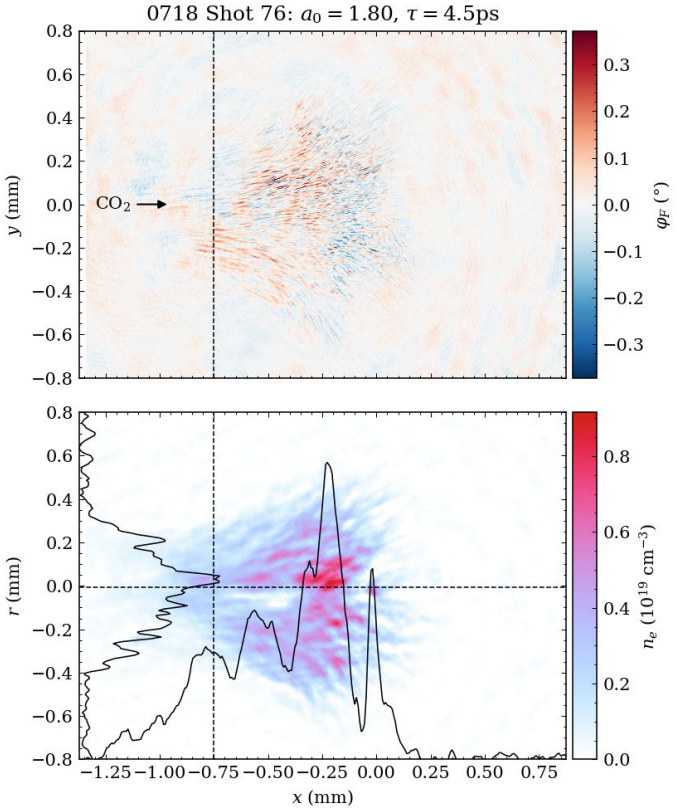

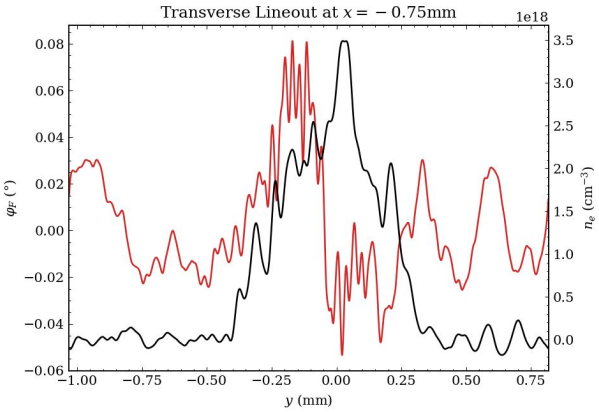

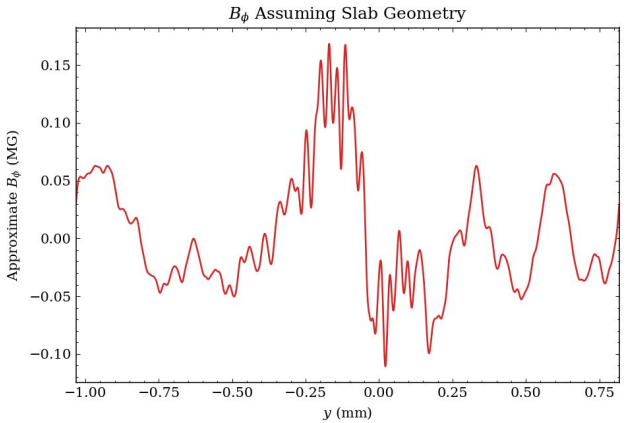

Shadowgraphs taken at higher densities show interesting structures.

These were taken using a shorter gas jet and higher backing pressure. The high density gradient resulted in loss of the probe due to diffraction in the center of the plasma. However, in several shots a clear beam of plasma can be seen clearly past the critical density surface.

Further study of these features requires a shorter wavelength probe to reduce loss due to diffraction.

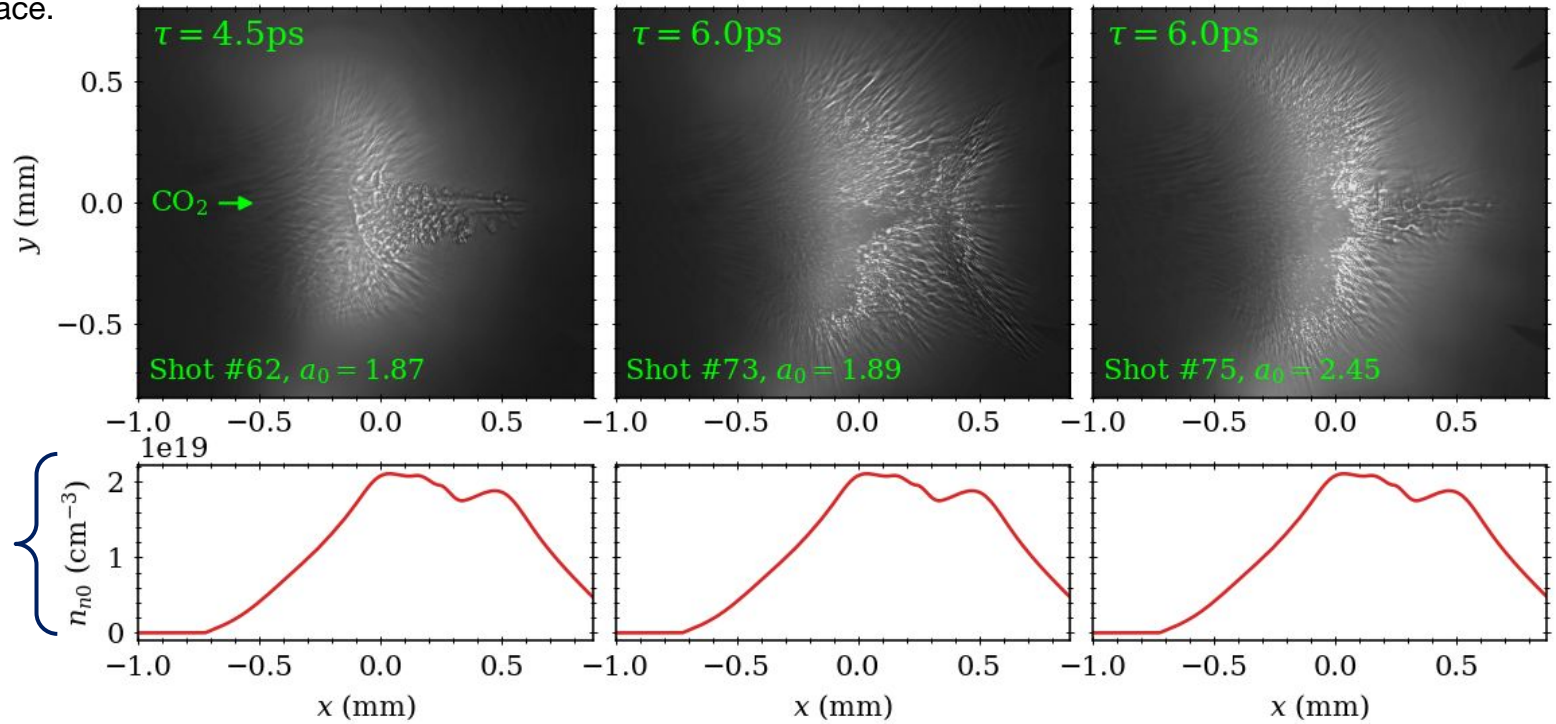

On-Axis Neutral Nitrogen Profile

Observed density and field structures are consistent with simulations.

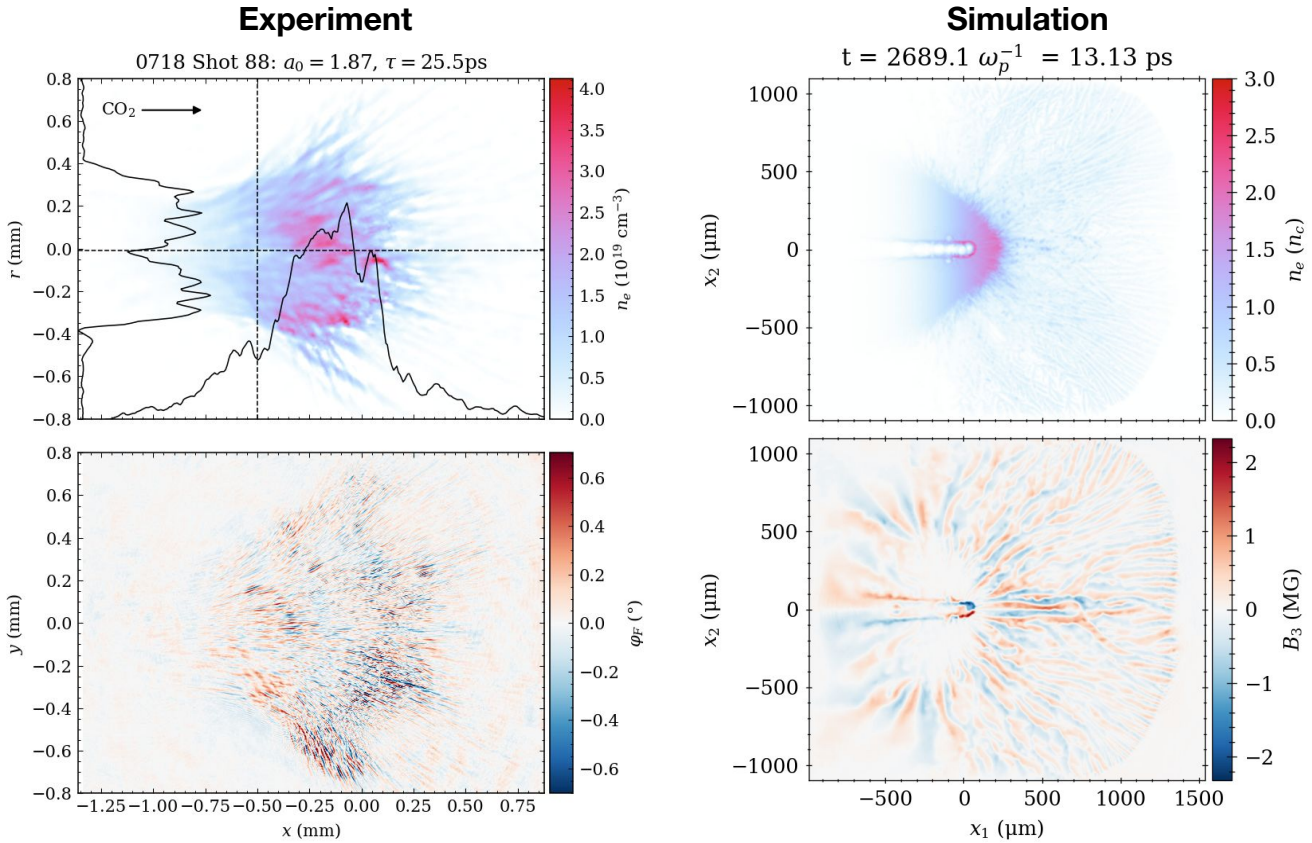

Simulations suggest ionization significantly impacts filamentation.

Simulation with Preionized Plasma

Simulation with Laser-Ionized Plasma

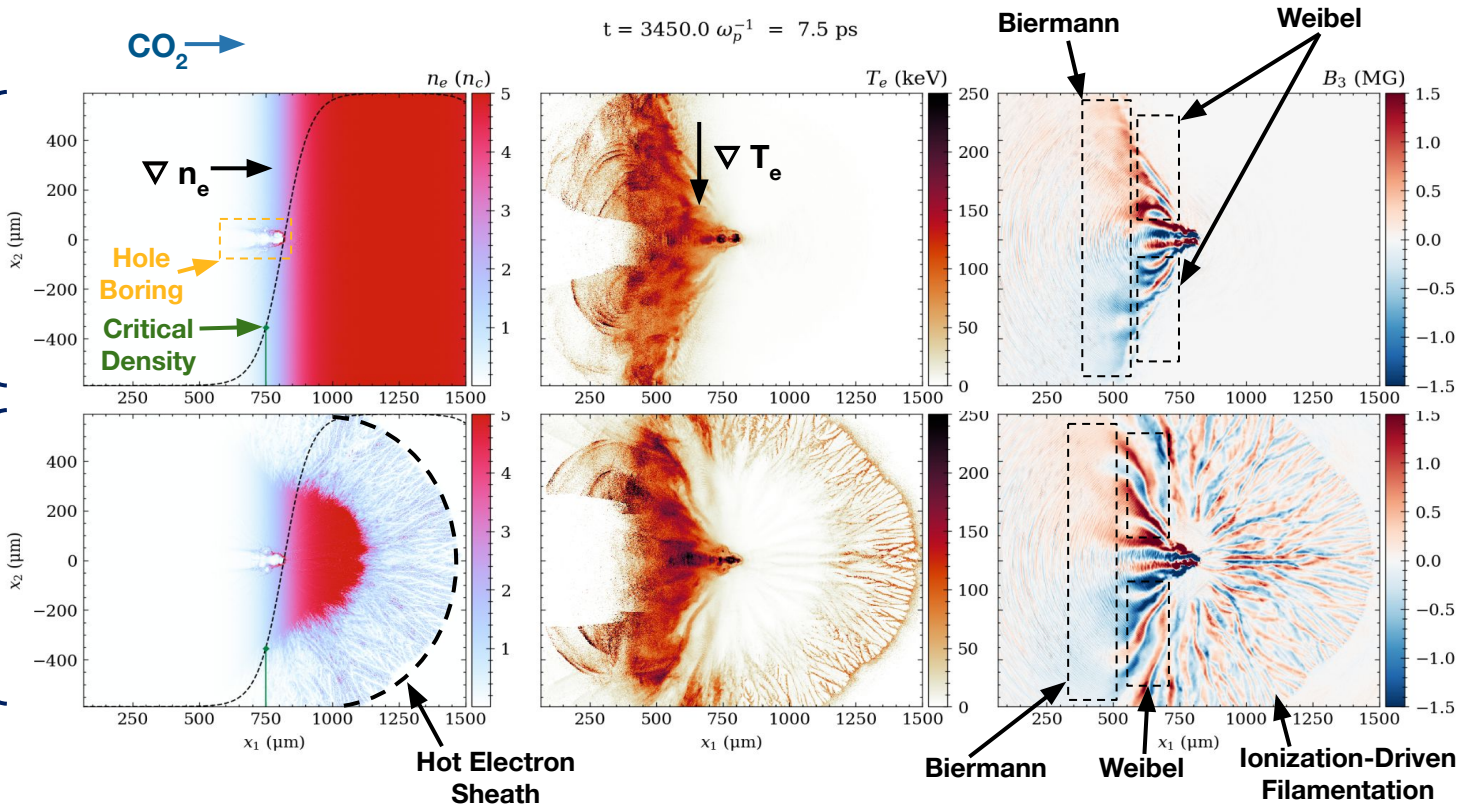

Plans for 2025

- Decrease the density gradient scale length using a blade or shock nozzle to reach Biermann dominated regime
- Observe overdense filamentation using a frequency doubled Ti:Sapphire probe to minimize diffraction effects.
    - This will decrease the Faraday rotation due to magnetic fields by a factor of 4, but we can better observe the density structures through shadowgraphy
- If possible, verify the impact of ionization/space-charge effects by preionizing the gas jet using Ti:Sa or the CO_2 prepulse

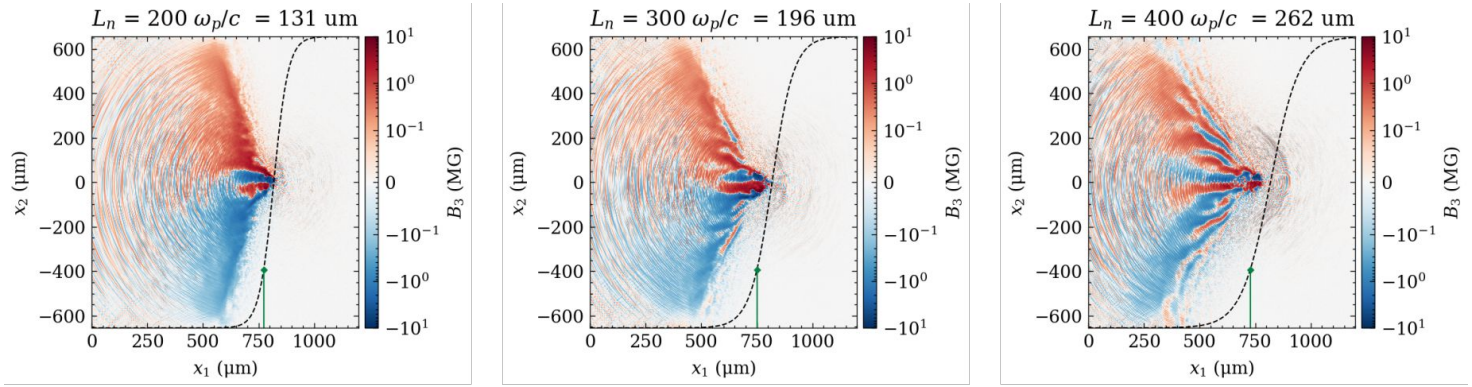

Summary

Experiment

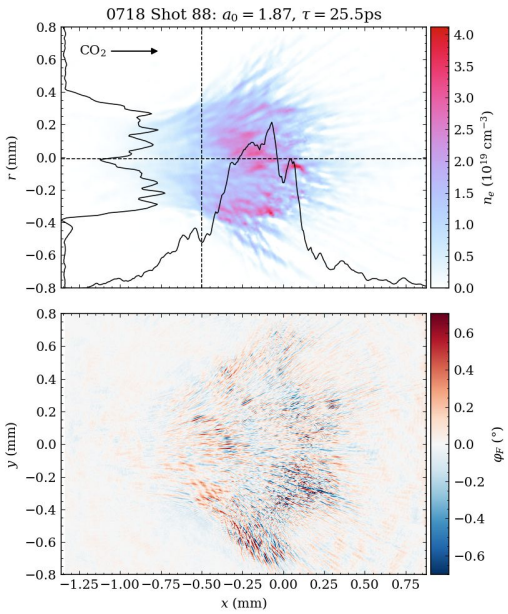

Simulation

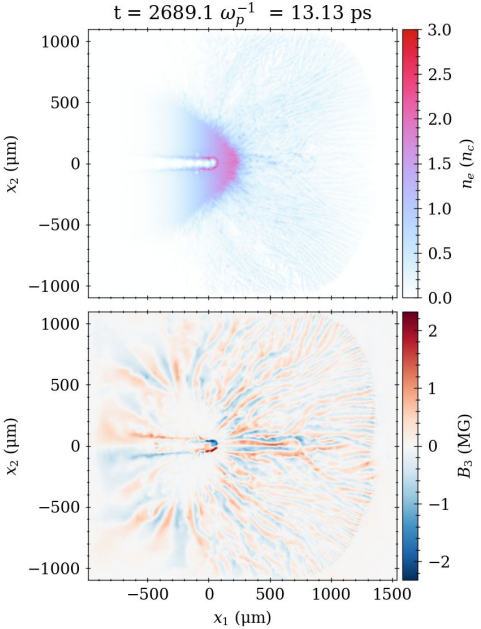

- Self-generated magnetic fields are significant to many fields of physics, such as ICF and astrophysical plasmas
- In overdense laser-plasma interactions, many different mechanisms can produce filamentation in both the magnetic field and the density, many of which are coupled together
- We have observed such filamentation in a near-critical density plasma via Faraday rotation and interferometry
- Computational studies suggest that the ionization process is dominating the structures observed and maintaining current filaments over long time scales

Electron Beam Requirements

Parameter	Units	Typical Values	Comments	Requested Values
Beam Energy	MeV	50-65	*Full range is ~15-75 MeV with highest beam quality at nominal values*	
Bunch Charge	nC	0.1-2.0	*Bunch length & emittance vary with charge*	
Bunch Length	ps	1-10	*Bunch charge & emittance vary with length*	
Peak current	A	100	*Variable with bunch charge and length*	
Compression	fs	Down to 100 fs (up to 1 kA peak current)	*A magnetic bunch compressor available to compress bunch down to ~100 fs. Beam quality is variable depending on charge and amount of compression required.* *NOTE: Further compression options are being developed to provide bunch lengths down to the ~10 fs level*	
Focused transverse size at IP (σ)	μm	30 – 100 (dependent on IP position)	*It is possible to achieve transverse sizes below 10 um with special permanent magnet optics.*	
Normalized Emittance	μm	1 (at 0.3 nC)	*Variable with bunch charge*	
Rep. Rate (Hz)	Hz	1.5	*3 Hz also available if needed*	
Trains mode	---	Single bunch	*Multi-bunch mode available. Trains of 24 or 48 ns spaced bunches.*	

CO_2 Laser Requirements

Configuration	Parameter	Units	Typical Values	Comments	Requested Values
CO_2 Regen. Amplifier	Wavelength	µm	9.2	*Wavelength determined by mixed isotope gain media*	
	Peak Power	GW	~3		
	Pulse Mode	---	Single		
	Pulse Length	ps	2		
	Pulse Energy	mJ	6		
	Repetition Rate	Hz	1.5	*3 Hz also available if needed*	
CO_2 CPA Beam	Wavelength	µm	9.2	*Wavelength determined by mixed isotope gain media*	9.2
Note that delivery of full power pulses to the Experimental Hall is presently limited to Beamline #1 only.	Peak Power	TW	2-3	*Up to 5 TW operation will be available in a limited number of shots upon the user's request.*	2-5
	Pulse Mode	---	Single		Single
	Pulse Length	ps	2	*3-year development effort to achieve <500 fs at >10 TW and deliver to users is in progress.*	2
	Pulse Energy	J	~5	*10J will be available in a limited number of shots upon the user's request.*	2-5
	Strehl Ratio	---	~0.5	*Recommended conservative estimate subject to verification.*	0.5
	Repetition Rate	Hz	0.01	*Burst operation at up to 0.05 Hz for a limited period is possible upon user's request. This regime should be avoided to extend the lifetime of the HV spark gaps in the amplifier's PFN*	0.01
	Polarization		Linear	*Adjustable linear polarization along with circular polarization can be provided upon request*	Linear & Circular

Other Experimental Laser Requirements

Ti:Sapphire Laser System	Units	Stage I Values	Stage II Values	Comments	Requested Values
Central Wavelength	nm	800	800	*Stage I parameters are presently available and setup to deliver Stage II should be available summer 2025*	800
FWHM Bandwidth	nm	20	13		20
Compressed FWHM Pulse Width	fs	<50	<75	*Transport of compressed pulses will initially include a very limited number of experimental interaction points. Please consult with the ATF Team if you need this capability.*	75
Chirped FWHM Pulse Width	ps	≥50	≥50		
Chirped Energy	mJ	10	200		
Compressed Energy	mJ	7	~20	*20 mJ is presently operational with work underway this year to achieve our 100 mJ goal.*	5
Energy to Experiments	mJ	>4.9	>80		
Power to Experiments	GW	>100	>1000		

Nd:YAG Laser System	Units	Typical Values	Comments	Requested Values
Wavelength	nm	1064	*Single pulse*	
Energy	mJ	100		
Pulse Width	ps	14		
Wavelength	nm	532	*Frequency doubled*	
Energy	mJ	0.5		
Pulse Width	ps	10		

Special Equipment Requirements and Hazards

- Electron Beam
  - N/A
- CO_2 Laser
  - Linear and Circular Polarization
- Ti:Sapphire and Nd:YAG Lasers
  - No special configurations needed
- Hazards & Special Installation Requirements
  - Large installation (chamber, insertion device, etc.):
  - Cryogens:
  - Introducing new magnetic elements:
  - Introducing new materials into the beam path:
  - Any other foreseeable beam line modifications:

Experimental Time Request

CY2025 Time Request

Capability	Setup Hours	Running Hours
Electron Beam Only		
Laser* Only (in Laser Areas)	40	40
Laser* + Electron Beam		

Total Time Request for the Experiment remaining duration

Capability	Setup Hours	Running Hours
Electron Beam Only		
Laser* Only (in Laser Areas)	40	80
Laser* + Electron Beam		

* Laser = Near-IR or LWIR (CO_2) Laser

Backup: Details of Faraday Rotation Diagnostic

$$\phi_{\mathrm{rot}} = \frac{e}{2m_e c n_c^{\mathrm{probe}}} \int_{\mathcal{P}} n_e \vec{B}_\varphi \cdot d\vec{\ell}$$

For the MG magnetic fields seen in simulation, we expect Faraday rotation of an 800nm probe between .1-1°.

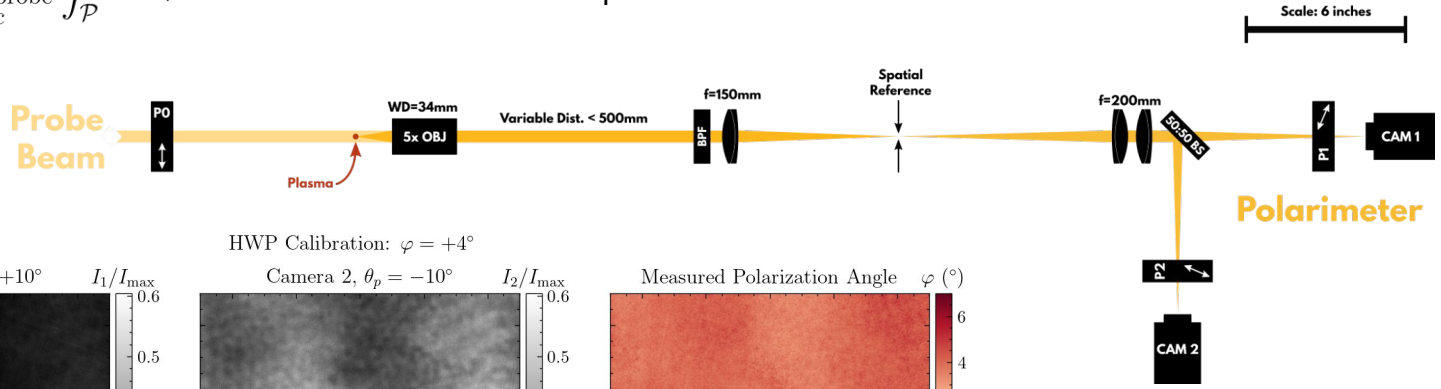

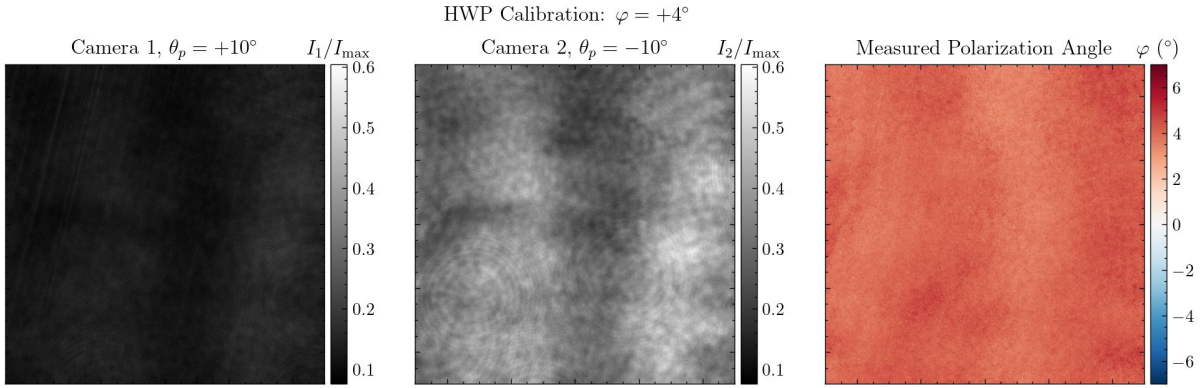

A two-camera differential measurement of polarization allows for sub-degree sensitivity while maintaining high spatial resolution.

Using a half-waveplate to rotate the probe polarization by a known angle demonstrates the accuracy of the imaging polarimeter.

Backup: Biermann Battery Theory

The Biermann battery effect generates magnetic fields in the presence of **nonparallel temperature and density gradients**

$$\frac{\partial \boldsymbol{B}}{\partial t} = \underbrace{\boldsymbol{\nabla} \times (\boldsymbol{v} \times \boldsymbol{B})}_{\text{Convection}} + \underbrace{\frac{\eta c^2}{4\pi} \boldsymbol{\nabla}^2 \boldsymbol{B}}_{\text{Diffusion}} - \underbrace{\frac{1}{en} \boldsymbol{\nabla} \times (\boldsymbol{j} \times \boldsymbol{B})}_{\text{Hall Effect}} - \underbrace{\frac{c}{n_e e} \boldsymbol{\nabla} n_e \times \boldsymbol{\nabla} T_e}_{\text{Biermann Battery}}$$

At early times the Biermann battery field is the only surviving term, growing linearly

$$B(t) \approx \frac{m_e c}{e} \frac{v_{the}^2}{L_n L_T} t, \quad L_n \equiv \frac{n_e}{\nabla n_e}, \quad L_T \equiv \frac{T_e}{\nabla T_e}$$

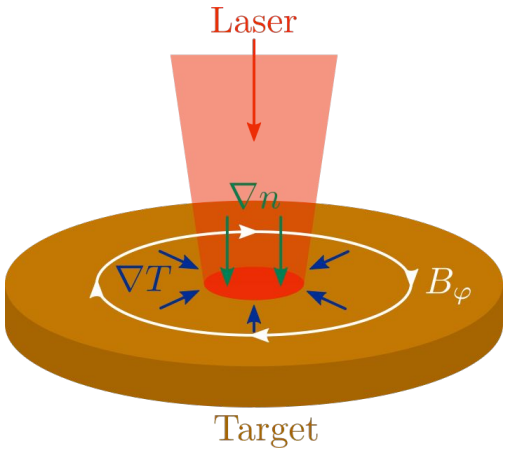

[S. I. Braginskii, *Rev. Plasma Phys.* 1, 205 (1965).]
[M. G. Haines, *Plasma Phys. Control. Fusion* 28, 1705 (1986).]
[A. Schekochihin and S. Cowley, *Magnetohydrodynamics* (2007).]

Backup: Weibel Instability Theory

The temperature gradients that contribute to the Biermann battery also create temperature anisotropy.

The Weibel instability grows in the presence of anisotropic temperatures.

For bi-Maxwellian velocity distributions:

$$1 - \frac{c^2 k^2}{\omega^2} + \frac{\omega_p^2}{\omega^2}\left[A + (A+1)\,\xi Z(\xi)\right] = 0, \quad \xi \equiv \frac{\omega}{\sqrt{2} k v_{\mathrm{cold}}}$$

$$A \equiv \frac{T_{\mathrm{hot}}}{T_{\mathrm{cold}}} - 1$$

Weibel instability admits a broad spectrum of unstable modes that coalesce towards a single mode as the plasma isotropizes.

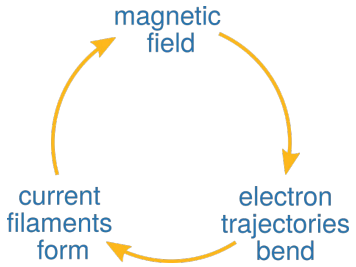

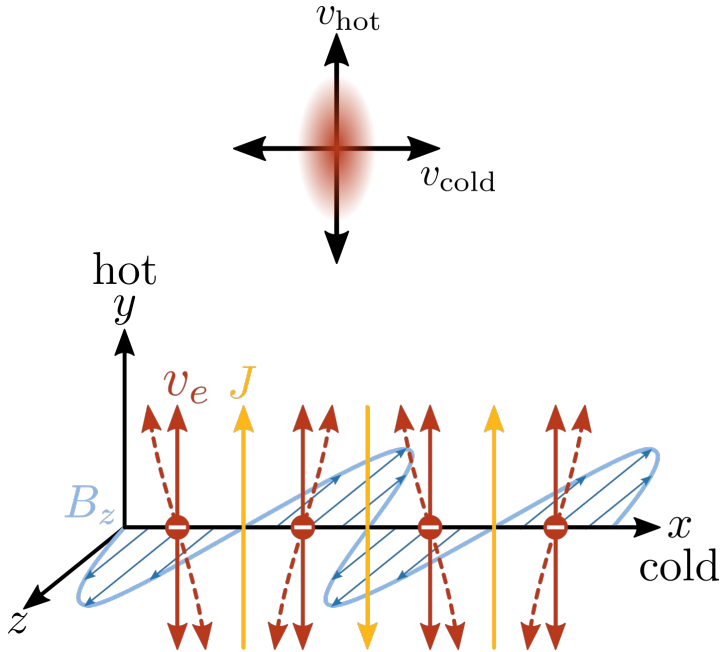

[Weibel, Phys. Rev. Lett. (1959)]
[Fried, Phys. Fluids (1959)]

Backup: Simulated Weibel & Biermann *k*-Space Evolution

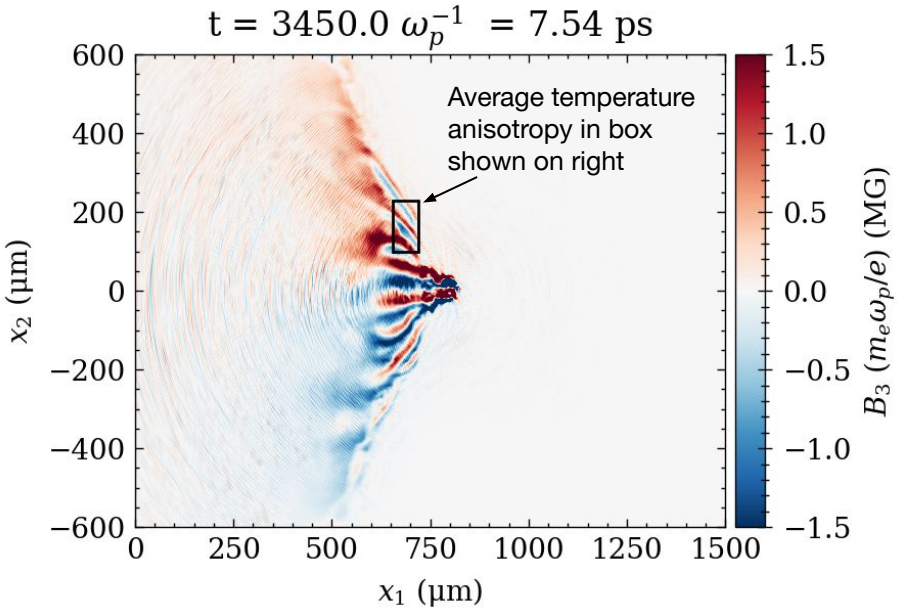

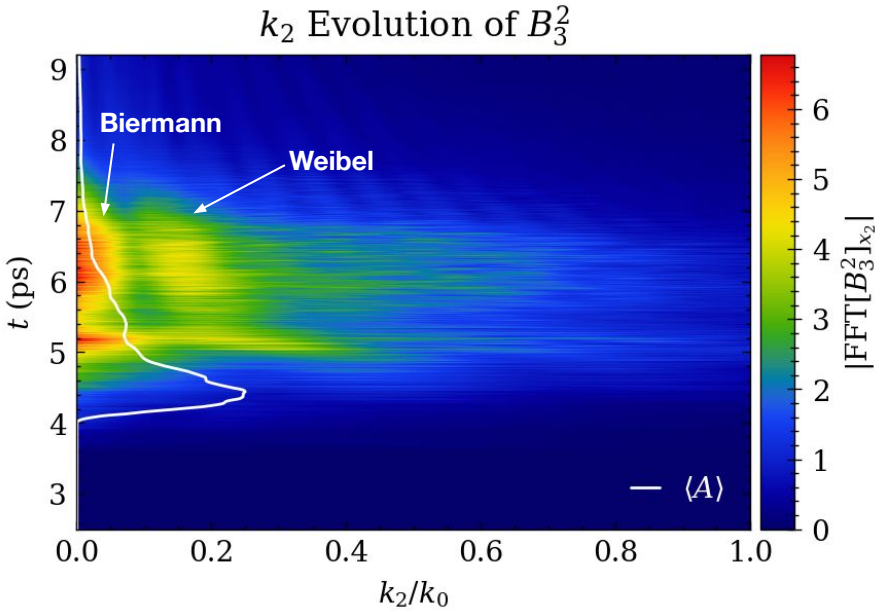

Backup: Measured phase shift from interferometry

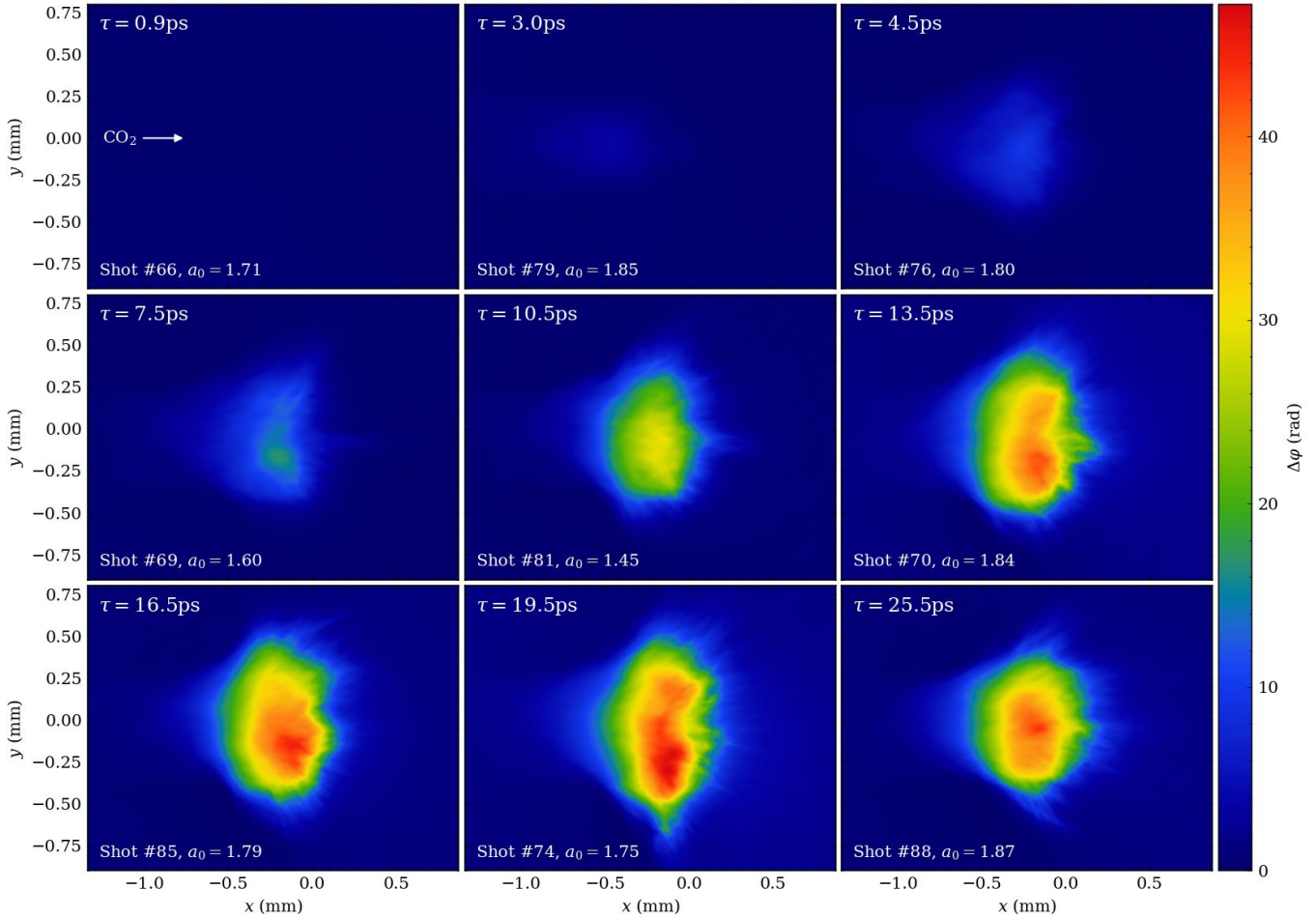

Backup: Analyzing the Plasma Density Filaments

Filaments in the plasma density aren't cylindrically symmetric about the laser axis, so we isolate them and treat them as a uniform slab on top of the bulk plasma.

$$\Delta\varphi(\vec{r}) = \frac{2\pi}{\lambda^{\text{probe}}}\int dz\ (\eta(\vec{r}) - 1) \approx -\frac{\pi}{\lambda^{\text{probe}}}\int dz\ \frac{n_e(\vec{r})}{n_c^{\text{probe}}}$$

$$n_e(\vec{r}) \approx n_r(x,\rho) + n_s(x,y), \quad \rho^2 \equiv y^2 + z^2 \longrightarrow \Delta\varphi(\vec{r}) \approx -\frac{\pi}{\lambda^{\text{probe}} n_c^{\text{probe}}}\{\mathcal{A}\left[n_r(x,\rho)\right] + n_s(x,y)s\}$$

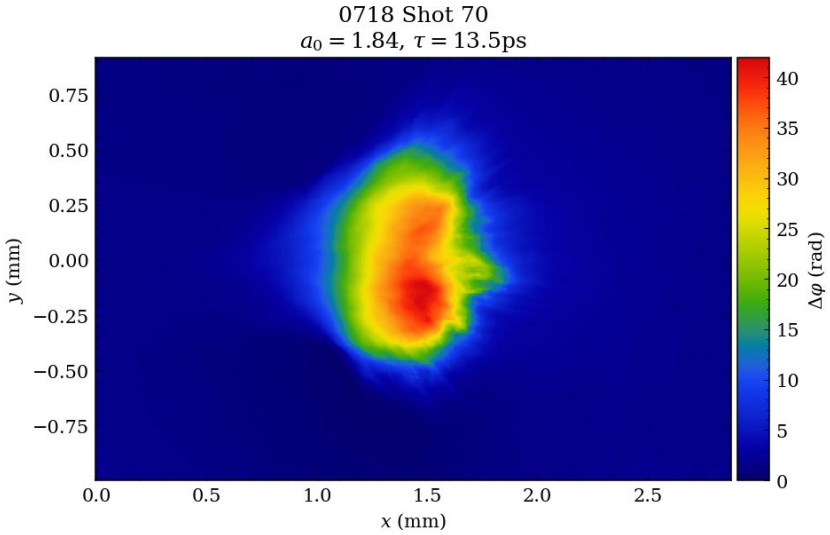

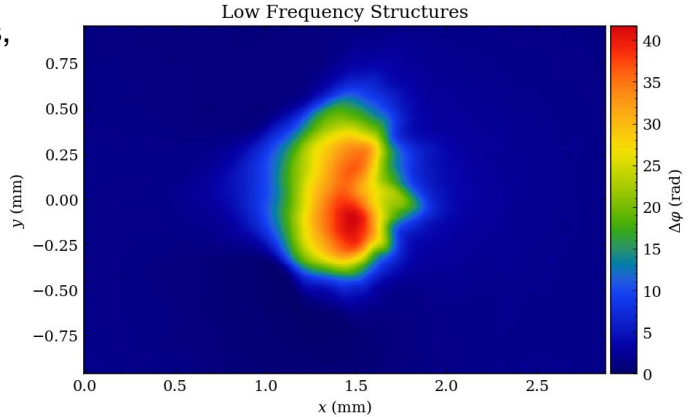

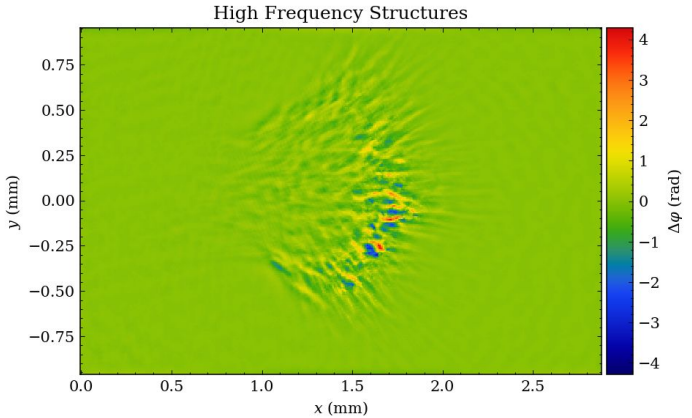

Backup: Reconstructed Density

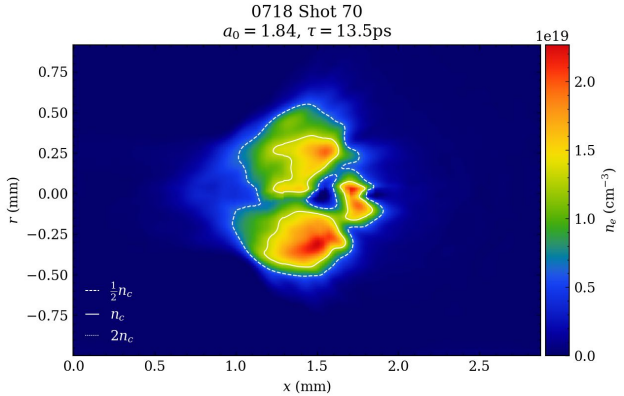

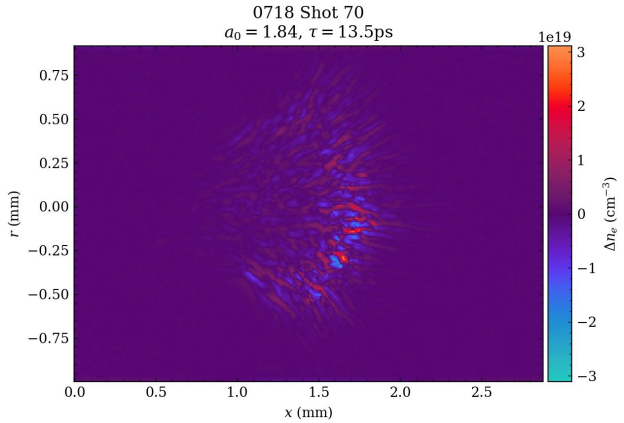

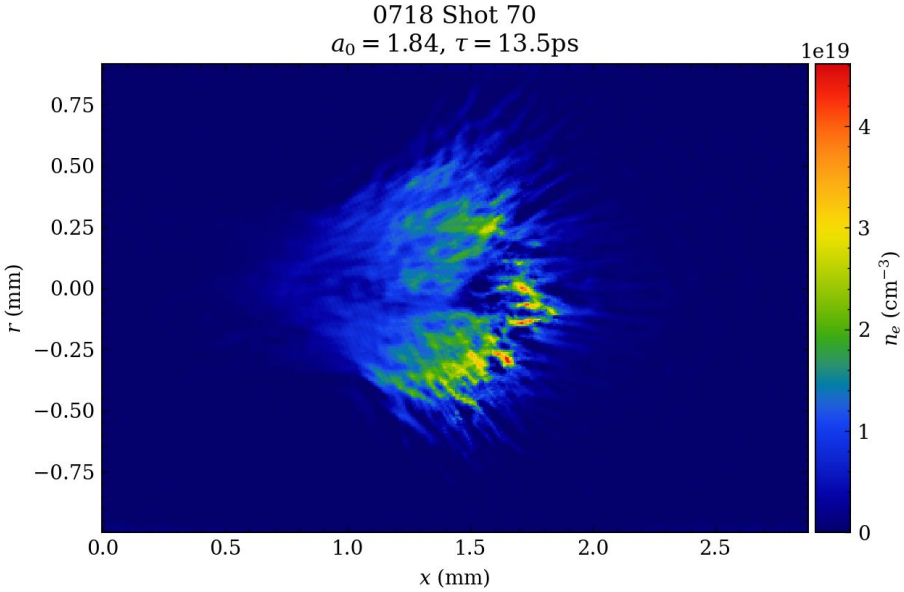

Backup: Movie of Simulated Biermann & Weibel in CO_2 Driven Plasma

2D OSIRIS simulations using laser parameters consistent with the CO_2 laser at BNL ATF (λ = 9.2μm, LP in x_3, a_0 = 2.0, 2.5 J, w_0 = 35μm, τ_{FWHM} = 2ps), incident on a preionized plasma with peak density $n_0 = 5n_c = 6.6 \cdot 10^{19} cm^{-3}$ and a density ramp characterized by $L_n = 300d_e$ = 196μm.